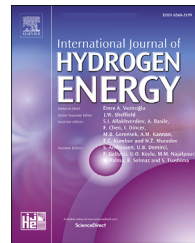


Available online at www.sciencedirect.com**ScienceDirect**journal homepage: www.elsevier.com/locate/he

Thermodynamic models for H₂O–CO₂–H₂ mixtures in near-critical and supercritical regions of water

Yuanbin Liu, Bingyang Cao*

Key Laboratory for Thermal Science and Power Engineering of Ministry of Education, Department of Engineering Mechanics, Tsinghua University, Beijing, 100084, China

HIGHLIGHTS

- The PVTx datasets of the H₂O–CO₂–H₂ mixtures are obtained by the MD simulations.
- Applicability of the DMW EOS for the ternary mixtures is evaluated.
- Missing mixing parameters of H₂O–H₂ and CO₂–H₂ are found for the DMW EOS.
- The DMW EOS is improved and optimized for the H₂O–CO₂–H₂ mixtures.

ARTICLE INFO

Article history:

Received 23 September 2019

Received in revised form

10 December 2019

Accepted 12 December 2019

Available online 9 January 2020

ABSTRACT

The PVTx properties of the H₂O–CO₂–H₂ mixtures have significant applications in the technology of supercritical water gasification of coal. Here, we first carry out the molecular dynamics simulations of the PVTx properties of the H₂O–CO₂–H₂ mixtures in the near-critical and supercritical regions of water to generate 600 datasets at 750–1150 K and 4.0–443.5 MPa. The molar fraction of each composition in the ternary mixtures ranges from 10% to 80%. Later we investigate the applicability of a well-known thermodynamic model for the ternary mixtures, namely the Duan-Møller-Weare equation of state (DMW EOS). It is observed that the DMW EOS shows great potential in the prediction of the PVTx properties of the ternary mixtures. However, it is noted that the mixing parameters describing the binary interactions of H₂O–H₂ and CO₂–H₂ are still unknown in the DMW EOS. By determining the missing mixing parameters using the Levenberg-Marquardt algorithm, the accuracy of the original DMW EOS is improved for the ternary mixtures. Moreover, optimizing the coefficients in the DMW EOS further promotes the accuracy of the model for the H₂O–CO₂–H₂ mixtures. The results from this work may facilitate the development of supercritical water gasification of coal.

© 2019 Hydrogen Energy Publications LLC. Published by Elsevier Ltd. All rights reserved.

Introduction

Energy crisis is one of the most prominent threats that modern people face. Discovering renewable energy and improving energy efficiency are helpful in easing the problem. Recently,

the technology of coal gasification in supercritical water shows significant promise for the remarkable improvement of energy efficiency and the sharp decrease of pollutant emissions [1–6]. The original products during coal gasification in supercritical water mainly include the mixtures CO₂–H₂. The

* Corresponding author.

E-mail address: caoby@tsinghua.edu.cn (B. Cao).

<https://doi.org/10.1016/j.ijhydene.2019.12.084>

0360-3199/© 2019 Hydrogen Energy Publications LLC. Published by Elsevier Ltd. All rights reserved.

$\text{H}_2\text{O}-\text{CO}_2-\text{H}_2$ mixtures are then purified and transferred from a gasifier to a steam turbine to generate electricity with zero net carbon emissions [1,3]. To date, much effort has been devoted to the development of coal gasification in supercritical water. Hydrogen production in various supercritical water gasification systems has been experimentally and systematically studied [7–12]. The effects of main operation parameters (temperature, pressure, flow rate, catalyst, oxidant, concentration of coal slurry) upon gasification have also been revealed [7–12]. Notably, the PVTx properties of the $\text{H}_2\text{O}-\text{CO}_2-\text{H}_2$ mixtures in the near-critical and supercritical regions of water are of considerable importance for the valid utilization of the technology [13]. Moreover, H_2O , CO_2 , and H_2 , as most common substances in both nature and industry, the PVTx properties of their mixtures have great potential applications in thermochemical processes [14] and environmental engineering [15].

Until now, abundant works have reported the thermodynamic properties of pure fluids for H_2O , CO_2 , and H_2 in the near-critical and supercritical regions by experimental measurements and numerical simulations [16–21]. There are also a wealth of researches about the PVTx properties and heat capacities of the binary mixtures of H_2O and CO_2 due to their specific applications in geochemical systems [15,21–23]. To the best of our knowledge, however, there are few studies reporting the datasets about the PVTx properties of the $\text{H}_2\text{O}-\text{CO}_2-\text{H}_2$ mixtures in the near-critical and supercritical regions of water. To obtain the datasets, experimental measurements are obviously preferred, while experiments under high TP conditions require high cost. As an alternative method, molecular dynamics (MD) simulations can effectively produce the PVTx data of the ternary mixtures in the near-critical and supercritical regions of water at a low cost. Dozens of works have indicated that the accuracy of MD simulations is comparable with that of experiments provided that the force fields are properly chosen [17,21,24]. Recently, the thermal conductivity [25] and viscosity [26] of the $\text{H}_2\text{O}-\text{CO}_2-\text{H}_2$ mixtures in the near-critical and supercritical regions of water have been numerically studied by the MD simulations. In our previous work, a few data about the PVTx properties of the $\text{H}_2\text{O}-\text{CO}_2-\text{H}_2$ mixtures in the near-critical and supercritical regions of water have been provided by using MD simulations [27].

It is impractical to generate data by experiments or MD simulations under all types of conditions due to pretty high cost and long calculation times. Therefore, a strong equation of state (EOS) is essential to correlate the data from experiments and MD simulations, which can be used to predict the thermodynamic behaviors of the ternary mixtures in the regions where both experimental and simulated data are not yet available. Historically, numerous researchers have been attracted to develop thermodynamic models for pure fluids and mixtures. Thus, dramatic progress has been made. Among these theoretical models, there is a remarkable and widely applied equation of state for thermodynamic calculations of the polar systems containing water under high-pressure conditions: the Duan-Møller-Weare (DMW) EOS [28]. Over the past few decades, the thermodynamic model has undergone considerable development [17,22]. However, there are few studies reporting the mixing parameters

describing the binary interactions for $\text{H}_2\text{O}-\text{H}_2$ and CO_2-H_2 , which may have a prominent effect on the performance of the DMW EOS for the $\text{H}_2\text{O}-\text{H}_2$, CO_2-H_2 , and $\text{H}_2\text{O}-\text{CO}_2-\text{H}_2$ mixtures.

The main objective of this work is to build a primary database and find a strong EOS for predicting the PVTx properties of the $\text{H}_2\text{O}-\text{CO}_2-\text{H}_2$ mixtures in the near-critical and supercritical regions of water. In Section [Methodology and theoretical background](#), we explain the technical details of MD simulations and carefully check the validity of the potential models for H_2O , CO_2 , and H_2 to guarantee the accuracy of MD simulations. Besides, the DMW EOS is introduced briefly. In Section [Results and discussion](#), we evaluate the accuracy of the classical DMW model for the $\text{H}_2\text{O}-\text{CO}_2-\text{H}_2$ mixtures in the near-critical and supercritical regions of water. By using the Levenberg-Marquardt optimization algorithm, the missing mixing parameters describing the binary interactions for $\text{H}_2\text{O}-\text{H}_2$ and CO_2-H_2 are determined. Moreover, the coefficients in the DMW EOS are optimized to further improve the accuracy of the model for the ternary mixtures. Sequentially, a thermodynamic model with high accuracy is found for the $\text{H}_2\text{O}-\text{CO}_2-\text{H}_2$ mixtures in the near-critical and supercritical regions of water. Conclusions are presented in Section [Conclusions](#).

Methodology and theoretical background

Simulation details

Interaction potentials of molecules play an extremely significant role in the molecular-level simulations. The $\text{H}_2\text{O}-\text{CO}_2-\text{H}_2$ mixtures contain three kinds of interactions between like molecules and three kinds of interactions between unlike molecules. Thanks to the numerous efforts devoted to the development of the accurate potential models, there are many successful potential models for pure fluids of H_2O , CO_2 , and H_2 . To describe the molecular interactions of water, there are famous SPC [29], SPC/E [30], TIP4P [31], and TIP4P-2005 [32] models. As to CO_2 , the most popular potential models are MSM [33], EPM2 [34], and TRAPP [35]. The single-site [36] and two-site [37] models are most common potential models for H_2 . In this work, we adopt the SPC/E model to investigate its performance in the MD simulations of the PVT properties of water. Due to their widest applications, EPM2 and two-site models are chosen for CO_2 and H_2 , respectively. Based on the similarity of $\text{H}_2\text{O}-\text{H}_2\text{O}$, CO_2-CO_2 , and H_2-H_2 potential models, the atomic pair interaction potentials for the $\text{H}_2\text{O}-\text{CO}_2-\text{H}_2$ mixtures can be written as a summation of short-range interactions between atoms and Coulombic interactions between charges:

$$u_{ij} = \sum_{m \in \{i\}} \sum_{n \in \{j\}} \left\{ 4\epsilon_{mn} \left[\left(\frac{\sigma_{mn}}{r_{mn}} \right)^{12} - \left(\frac{\sigma_{mn}}{r_{mn}} \right)^6 \right] + \frac{q_m q_n}{4\pi\epsilon_0 r_{mn}} \right\} \quad (1)$$

where u_{ij} is the interaction potential between molecules i and j ; m and n are the atoms of the molecules i and j , respectively; ϵ_{mn} and σ_{mn} denote the energy and size parameters for the short-range Lennard-Jones potential, respectively; r_{mn} is the distance between the interaction sites; q_m and q_n are the

partial charges designated on the interaction sites; ϵ_0 is the dielectric constant of vacuum. For like molecules $i = j$, the parameters in Eq. (1) are directly obtained from corresponding potential models of pure fluids. For unlike molecules $i \neq j$, the parameters in Eq. (1) can be calculated by the usual Lorentz–Berthelot [38] and the Kong [39] combining rules. In this work, we adopt the Lorentz–Berthelot rule due to its simplicity of expressions: $\epsilon_{mn} = \sqrt{\epsilon_m \epsilon_n}$ and $\sigma_{mn} = (\sigma_m + \sigma_n)/2$. It is worth noting that there is the additional bond stretching potential besides the potentials in Eq. (1) for the flexible EPM2 model: $u_\theta = k_\theta(\theta - \theta_0)^2/2$, where k_θ is the bond bending force constant; θ is the flexible bond angle of CO₂; θ_0 is 180°. Table 1 shows the involved force field parameters, where k_B is the Boltzmann constant and 'l' represents the bond length.

A series of MD simulations are performed by using the LAMMPS package [40]. Simulated systems contain 1000 molecules for pure fluids and more than 1000 molecules for mixtures. More specially, 2500 molecules are adopted for the simulations of the H₂O–CO₂–H₂ mixtures. All molecules are located in a cubic box with periodic boundary conditions. The long-range Coulombic interactions are handled by the particle-particle/particle-mesh (PPPM) whereas the short-range interaction potential is cut off beyond 12 Å. A Nosé–Hoover thermostat [41] is coupled to systems to control temperatures for the canonical (NVT) ensembles. For the isothermal-isobaric (NPT) ensembles, an additional Nosé–Hoover barostat [42] is applied to control pressures of systems besides a Nosé–Hoover thermostat. The pressure of systems is calculated along the NVT ensembles, while the volumetric properties of systems are simulated along the NPT ensembles. The time step is of 1 fs in all simulations. Initial equilibration periods are 50 ps and 600 ps for pure fluids and mixtures, followed by simulation runs of 400 ps and 600 ps to record meaningful data, respectively.

Duan-Møller-Weare equation of state

Compared with the cubic equations of state, the DMW EOS has a more complicated form with fourteen coefficients [17]:

$$Z = \frac{P_z v_z}{RT_z} = 1 + \frac{a_1 + a_2/T_z^2 + a_3/T_z^3}{v_z} + \frac{a_4 + a_5/T_z^2 + a_6/T_z^3}{v_z^2} + \frac{a_7 + a_8/T_z^2 + a_9/T_z^3}{v_z^4} + \frac{a_{10} + a_{11}/T_z^2 + a_{12}/T_z^3}{v_z^5} + \frac{a_{13}}{T_z^3 v_z^2} \left(1 + \frac{a_{14}}{v_z^2}\right) \exp\left(-\frac{a_{14}}{v_z^2}\right) \quad (2)$$

with

$$P_z = \frac{3.0626\sigma^3 P}{\epsilon} \quad (3)$$

$$T_z = \frac{154T}{\epsilon} \quad (4)$$

$$v_z = \frac{v}{1000} \left(\frac{\sigma}{3.691}\right)^{-3} \quad (5)$$

where Z is the compression factor; the coefficients a_1 – a_{14} and the Lenard–Jones potential parameters ϵ , σ for different pure species can be found in Ref. [17]; v is in cm³/mol and P in bar whereas T in K and R = 0.08314467. For mixture applications of the DMW EOS, the Lorentz–Berthelot rules are used to mix the parameters ϵ and σ [17]:

$$\epsilon = \sum_i \sum_j x_i x_j C_{1,ij} \sqrt{\epsilon_i \epsilon_j} \quad (6)$$

$$\sigma = \sum_i \sum_j x_i x_j C_{2,ij} (\sigma_i + \sigma_j)/2 \quad (7)$$

where $C_{1,ij}$ and $C_{2,ij}$ are the mixing parameters describing the binary interaction between components i and j. Both $C_{1,ij}$ and $C_{2,ij}$ are empirical parameters, which can be regarded as a correction of the deviation between the EOS prediction and experimental data. For like molecules ($i = j$), both $C_{1,ij}$ and $C_{2,ij}$ are equal to 1. If $i \neq j$, $C_{1,ij} = 0.84$ and $C_{2,ij} = 1.03$ are available for the H₂O–CO₂ mixtures [17], whereas both them are unknown for the H₂O–H₂ and CO₂–H₂ mixtures.

Results and discussion

Reliability of MD simulations

In MD simulations, an initial and crucial step is to select a good potential model to guarantee that the simulations can fairly reproduce the thermodynamic properties of computed systems. In this section, we first check the reliability of the SPC/E model by comparing its calculation results with available experimental data for the volumetric properties of pure water as shown in Table 2. It is observed that the results from the potential model agree well with experimental data. For the mixtures of H₂O and CO₂, we adopt the EPM2 model for CO₂ combined with the SPC/E potential model for H₂O to check their reliability in the volumetric simulations of systems. The results are shown in Table 3. An overall good agreement is observed between the simulated results and experimental data. The deviations of the MD simulations from the experimental data may mainly arise from the simplification of the

Table 1 – Parameters and geometries for different potential models.

Model	$\epsilon/k_B(K)$	$\sigma(\text{\AA})$	$q(e)$	$l(\text{\AA})$	$\theta_0(^{\circ})$	$k_\theta(\text{kJ/mol}\cdot\text{rad}^2)$
SPC/E	78.1845 (O)	3.166 (O)	-0.8476(O) 0.4238(H)	1.0(OH)	109.47(HOH)	–
EPM2	28.129 (C)	2.757 (C)	0.6512(C)	1.149(CO)	180(OCO)	1236
	80.507 (O)	3.033 (O)	-0.3256(O)			
Two-site	10 (H)	2.72 (H)	0(H)	0.74(HH)	–	–

Table 2 – Comparison between the simulated and experimental PVT data of H₂O.

T (K)	P (MPa)	v (cm ³ /mol)	
		SPC/E	Exp.
673.15	2000	14.89 (0.09)	14.97 [20]
983.15	1850	16.78 (0.13)	16.98 [19]
1203.15	950	22.33 (0.29)	22.56 (0.36) [16]
1491.15	950	25.43 (0.38)	25.86 (0.61) [16]
1493.15	1750	20.03 (0.22)	20.49 (0.24) [16]

Table 3 – Comparison between the simulated and experimental PVTx data of the H₂O–CO₂ mixtures.

T (K)	P (MPa)	x _{CO₂}	v (cm ³ /mol)	
			MD	Exp.
588.5	17.05	0.3983	235.90 (0.14)	225.65 [18]
606.61	18.04	0.3983	236.53 (0.15)	225.89 [18]
633.88	19.473	0.3983	237.62 (0.13)	226.24 [18]
1473.15	950	0.218	29.95 (.02)	29.07 (.73) [44]
1473.15	950	0.413	33.85 (.01)	32.95 (.78) [44]
1473.15	950	0.606	37.65 (.01)	36.47 (.83) [44]
1573.15	1450	0.128	24.39 (.01)	24.31 (.35) [44]
1573.15	1450	0.205	26.04 (.01)	25.51 (.41) [44]
1573.15	1450	0.387	29.27 (.01)	28.61 (.41) [44]
1673.15	1450	0.237	27.39 (.01)	26.78 (.48) [44]
1673.15	1450	0.39	30.07 (.01)	29.65 (.48) [44]
1673.15	1450	0.45	30.96 (.01)	30.37 (.46) [44]

combing rules and the precision of the potential models. The SPC/E model for H₂O and the two-site model for H₂ are employed to calculate the excess volumes for the mixtures of H₂O and H₂ as shown in Table 4. It shows that our MD simulations can generally reproduce the excess volumes of the H₂O–H₂ mixtures with the average absolute relative deviation of 10.86%. It is worth noting that carrying out such an experiment working with hydrogen at high temperatures and pressures is rather difficult. The experimental errors may mainly arise from the hydrogen leakage and the hydrogen embrittlement of the pressure transducers. Moreover, Seward et al. [43] indicated that excess thermodynamic properties are rather sensitive to weakly anisotropic intermolecular forces from multipoles of both hydrogen and water. In this case, we think that the average deviation of 10.86% between the MD simulations and the experiment for the excess volumes of the

H₂O–H₂ binary mixtures may be reasonable and acceptable. Finally, the validity of the two-site model for H₂ is checked as shown in Table 5. All MD simulated results are comparable to those of experiments, which validates the accuracy of our simulation method. In this work, we adopt the parameters of the SPC/E, EPM2, and two-site models to the calculations of the H₂O–CO₂–H₂ ternary mixtures.

Applicability of the DMW EOS and its improvement

In this section, we first illustrate the accuracy of the original DMW EOS for the ternary mixtures by comparison with the MD simulations. The coefficients a_{11} – a_{14} in the original DMW EOS are exhibited in Table 6. The known mixing parameters describing the binary interaction for H₂O–CO₂ are shown in Table 7. For the unknown mixing parameters, we set them to 1.0 to perform the calculation of the original DMW EOS. Details regarding the 600 simulated datasets of the PVTx properties of the H₂O–CO₂–H₂ mixtures are shown in Table 8. For more direct comparison between the DMW EOS calculations and the MD simulations, we define the absolute relative deviations as:

$$\text{ARD} = \left| \frac{P_{\text{MD}} - P_{\text{EOS}}}{P_{\text{MD}}} \right| \times 100\% \quad (8)$$

where the subscripts ‘MD’ and ‘EOS’ represent the MD simulations and the EOS calculations, respectively. Fig. 1 illustrates the relative deviations of the original DMW EOS for predicting the pressure of the ternary mixtures in the near-critical and supercritical regions of water. The performance of the original DMW EOS is remarkable with the average absolute relative deviation (AARD) of 2.55%. As shown in Table 8, however, it is also observed that the maximum deviation of the original DMW EOS reaches 13.87% in the case of T = 750 K, v = 0.1 L/mol and x_{H₂} : x_{CO₂} : x_{H₂} = 8 : 1 : 1. The maximum deviation of the original DMW EOS occurs when the system is water-rich and its temperature approaches the critical temperature of water. The observed result is consistent with that of Ref. [17]. Although the original DMW EOS has demonstrated great potential to predict the PVTx properties of the ternary mixtures, it is better to further improve the accuracy of the model.

Determining the missing mixing parameters describing the binary interactions of H₂O–H₂ and CO₂–H₂ is an intuitive way to improve the DMW EOS. Estimating the mixing parameters

Table 4 – Comparison between the simulated and experimental excess volumes of the H₂O–H₂ mixtures for a set of pressures at T = 673.15 K and x_{H₂} = 0.5.

P (MPa)	v ^{ex} (cm ³ /mol)	
	MD	Exp [43]
30	45.13	50.0
40	30.64	33.7
60	15.71	17.7
100	6.04	6.6
150	2.81	3.1
200	1.64	1.4
250	1.11	1.0

Table 5 – Comparison between the simulated and experimental PVT data of H₂. NIST denotes the National Institute of Standards and Technology, which produces the standard reference data on the thermodynamic and transport properties of fluids.

T (K)	P (MPa)	v (cm ³ /mol)		
		Two-site	Exp [45]	NIST
373.15	500	20.22 (0.01)	20.21	20.12
373.15	600	18.83 (0.01)	18.75	18.67
373.15	700	17.77 (0.01)	17.62	17.56
423.15	500	21.16 (0.01)	21.01	20.97
423.15	600	19.62 (0.01)	19.70	19.39
423.15	700	18.47 (0.01)	18.17	18.19

Table 6 – Original and optimized coefficients in the DMW EOS.

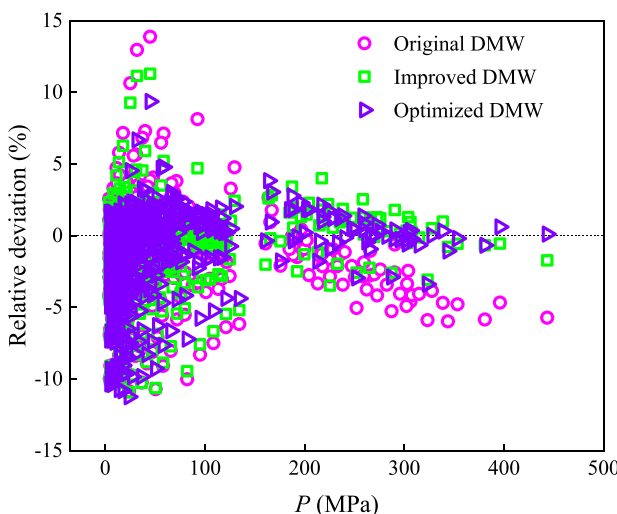
	Original [17]	Optimized
a_1	$3.75504388 \times 10^{-2}$	$4.10531320 \times 10^{-2}$
a_2	-1.08730273×10^4	-1.37620027×10^4
a_3	1.10964861×10^6	1.10962302×10^6
a_4	$5.41589372 \times 10^{-4}$	$1.83220339 \times 10^{-4}$
a_5	1.12094559×10^2	7.76316432×10^2
a_6	-5.92191393×10^3	-6.00607402×10^3
a_7	$4.37200027 \times 10^{-6}$	$-7.17876288 \times 10^{-7}$
a_8	$4.95790731 \times 10^{-1}$	1.03984715×10^0
a_9	-1.64902948×10^2	-1.90542029×10^3
a_{10}	$-7.07442825 \times 10^{-8}$	$2.71261934 \times 10^{-7}$
a_{11}	$9.65727297 \times 10^{-3}$	$-1.33478326 \times 10^{-1}$
a_{12}	$4.87945175 \times 10^{-1}$	1.04348186×10^2
a_{13}	1.62257402×10^4	1.62266317×10^4
a_{14}	$8.99000000 \times 10^{-3}$	$4.66699733 \times 10^{-1}$

Table 7 – Original and newly obtained mixing parameters describing the binary interactions in the DMW EOS.

	Original [17]		Newly obtained	
	$C_{1, ij}$	$C_{2, ij}$	$C_{1, ij}$	$C_{2, ij}$
H ₂ O–CO ₂	0.84	1.03	/	/
H ₂ O–H ₂	/	/	1.57	1.04
CO ₂ –H ₂	/	/	1.10	1.07

Table 8 – Details regarding the simulated PVTx properties of the H₂O–CO₂–H₂ mixtures and the deviations of the original, improved, and optimized DMW EsOS.

Models	x _{H₂O}	x _{CO₂}	x _{H₂}	v (L/mol)	T (K)	P (MPa)	AARD	Max ARD
Original							2.55%	13.87%
Improved	0.1–0.8	0.1–0.8	0.1–0.8	0.05–1.5	750–1150	4.0–443.5	2.34%	11.29%
Optimized							2.27%	11.25%

**Fig. 1 – Comparison of the relative deviations of the original, improved, and optimized DMW EsOS for predicting the pressure of the H₂O–CO₂–H₂ mixtures in the near-critical and supercritical regions of water.**

can be formulated as an optimization problem for the minimization of the objective function:

$$F = \frac{1}{2} \left\{ \sum_{i=1}^N [P_{EOS,i}(T_i, v_i, x_{1,i}, x_{2,i}, x_{3,i}) - P_{MD,i}(T_i, v_i, x_{1,i}, x_{2,i}, x_{3,i})]^2 \right\}. \quad (9)$$

By using the Levenberg-Marquardt algorithm to fit the 600 datasets of the MD simulations for the ternary mixtures, the missing mixing parameters are determined and displayed in **Table 7**. Here, the DMW EOS adopting the newly obtained mixing parameters, the coefficients a_1 – a_{14} being held unchanged with the original model, is called the improved DMW EOS. The relative deviations of the improved DMW EOS are shown in **Fig. 1**. Compared with the original model, the accuracy of the improved DMW EOS is prominently increased in the high-pressure regimes. Simultaneously, it is shown that the maximum deviation is decreased from 13.87% using the original model to 11.29% using the improved model. It is implied that the missing mixing parameters cannot be disregarded for the H₂O–CO₂–H₂ mixtures. To further promote the accuracy of the DMW EOS for the ternary mixtures, one effective method is to modify the coefficients by global optimization algorithms. It is worth noting that this way may constitute a local thermodynamic model and reduce the generalization of the DMW EOS for other substances. The objective function of optimizing coefficients is also adopted as

Eq. (9). The optimized coefficients a_1 – a_{14} are obtained by the Levenberg-Marquardt algorithm as presented in **Table 6**. Here, the model adopting the optimized coefficients and the newly obtained mixing parameters is called the optimized DMW EOS. As a result, **Table 8** shows that the optimized DMW EOS with AARD of 2.27% exhibits the best overall performance among the three models for the H₂O–CO₂–H₂ mixtures in the near-critical and supercritical regions of water. The maximum deviation of the optimized DMW EOS is close to that of the improved DMW EOS, while the optimized DMW EOS has a better performance than the improved DMW EOS in the high-pressure regimes as shown in **Fig. 1**. Note that both the improved and optimized DMW models share the same equation form with the original DMW EOS.

It is interesting to explore the accuracy of the original, improved, and optimized DMW models for the H₂O–H₂ and CO₂–H₂ mixtures. This can be used to examine whether the newly obtained mixing parameters describing the binary interactions of H₂O–H₂ and CO₂–H₂ are conducive to promoting the accuracy of the original DMW EOS for the H₂O–H₂ and CO₂–H₂ mixtures. The PVTx properties of the H₂O–H₂ mixtures are obtained by the MD simulations, which yields 20

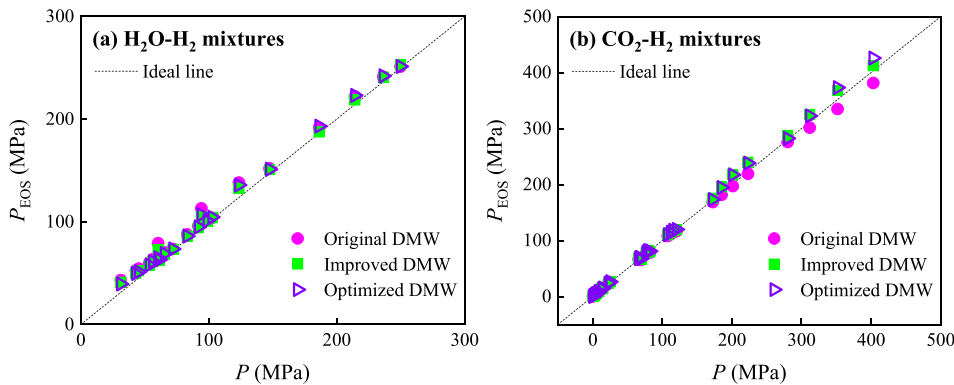


Fig. 2 – Accuracy of the original, improved, and optimized DMW EsOS for predicting the pressure of (a) the $\text{H}_2\text{O}-\text{H}_2$ mixtures and (b) the CO_2-H_2 mixtures. As to the $\text{H}_2\text{O}-\text{H}_2$ mixtures, all benchmarks are obtained by the MD simulations. For the CO_2-H_2 mixtures, the benchmarks consist of 20 simulated datasets and 16 experimental datasets [46].

datasets in the supercritical region of water. For the CO_2-H_2 mixtures, 20 datasets are obtained from the MD simulations and other 16 datasets are derived from the experimental measurements [46]. The results about the $\text{H}_2\text{O}-\text{H}_2$ and CO_2-H_2 mixtures are plotted in Fig. 2. It is shown that the optimized DMW EOS gives a better prediction with AARD of 6.77% than the original model with AARD of 10.15% and the improved DMW EOS with AARD of 7.04% for the $\text{H}_2\text{O}-\text{H}_2$ mixtures. For the CO_2-H_2 mixtures, the original, improved, and optimized models give the remarkable prediction precision with AARD below 2.5%. Both two newly obtained mixing parameters describing the binary interaction of CO_2-H_2 are close to 1 so that they have little influence on the overall accuracy of the DMW EOS for the CO_2-H_2 mixtures. However, it is observed that those two newly obtained mixing parameters are helpful to improve the accuracy of the original DMW EOS for the CO_2-H_2 mixtures in the high-pressure regimes. All above results illustrate that the mixing parameters are significant factors to improve the DMW EOS for the binary mixtures. Moreover, it is validated that the DMW model with optimized coefficients is still suitable for predicting the PVTx properties of the $\text{H}_2\text{O}-\text{H}_2$ and CO_2-H_2 mixtures.

Conclusions

The PVTx properties of the $\text{H}_2\text{O}-\text{CO}_2-\text{H}_2$ mixtures in the near-critical and supercritical regions of water are essential for the valid utilization of the coal gasification technology. We first obtain 600 PVTx datasets of the $\text{H}_2\text{O}-\text{CO}_2-\text{H}_2$ mixtures in the near-critical and supercritical regions of water by using molecular dynamics simulations, which can mitigate the data shortage of the PVTx properties of the ternary mixtures. Then we explore the applicability of the DMW EOS in predicting the PVTx properties of the $\text{H}_2\text{O}-\text{CO}_2-\text{H}_2$ mixtures in the near-critical and supercritical regions of water. The original DMW EOS presents remarkable predictability with the average absolute relative deviation of 2.55% and a maximum deviation of 13.87% for the ternary mixtures. As an improvement of the original DMW EOS, we determine the missing mixing parameters describing the binary interactions of $\text{H}_2\text{O}-\text{H}_2$ and CO_2-H_2 by using the Levenberg-Marquardt algorithm to fit the

simulated data of the ternary mixtures. It is shown that those missing mixing parameters are significant factors to enhance the accuracy of the original model for the CO_2-H_2 , $\text{H}_2\text{O}-\text{H}_2$, and $\text{H}_2\text{O}-\text{CO}_2-\text{H}_2$ mixtures. Moreover, we optimize the coefficients of the original DMW EOS based on the thermodynamic datasets of the $\text{H}_2\text{O}-\text{CO}_2-\text{H}_2$ mixtures in the near-critical and supercritical regions of water, which is demonstrated to be effective to further improve the accuracy of the model for the ternary mixtures. The results from this study may facilitate the application of the coal gasification in supercritical water and promote the development of the classical thermodynamic models.

Acknowledgments

This work is supported by the National Key R&D Program of China (Grant No. 2016YFB0600100).

Nomenclature

ARD	Absolute relative deviation
AARD	Average absolute relative deviation
DMW	Duan-Møller-Weare
EOS	Equation of state
F	Objective function
MD	Molecular dynamics
PPPM	Particle-particle/particle-mesh
a_1-a_{14}	Coefficients
C	Mixing parameter
k_B	Boltzmann constant
k_θ	Bond bending force constant
l	Bond length
N	Size of the PVTx datasets
P	Pressure
q	Partial charge
r	Distance between the interaction sites
T	Temperature
u	Interaction potential
V	Volume of the system
v	Molar volume
x	Mole fraction

Z Compression factor

Greek Symbols

ε	Energy parameter for the short-range Lennard-Jones potential
ϵ_0	Dielectric constant of vacuum
θ_0	Bond angle
σ	Size parameter for the short-range Lennard-Jones potential

Subscripts

EOS	EOS calculations
i	Component reference letter
j	Component reference letter
MD	MD simulations
m	Component reference letter
n	Component reference letter

Appendix A. Supplementary data

Supplementary data to this article can be found online at <https://doi.org/10.1016/j.ijhydene.2019.12.084>.

REFERENCES

- [1] Guo L, Jin H. Boiling coal in water: hydrogen production and power generation system with zero net CO₂ emission based on coal and supercritical water gasification. *Int J Hydrogen Energy* 2013;38:12953–67.
- [2] Lan R, Jin H, Guo L, Ge Z, Guo S, Zhang X. Hydrogen production by catalytic gasification of coal in supercritical water. *Energy Fuels* 2014;28:6911–7.
- [3] Guo L, Jin H, Lu Y. Supercritical water gasification research and development in China. *J Supercrit Fluids* 2015;96:144–50.
- [4] Rodriguez Correa C, Kruse A. Supercritical water gasification of biomass for hydrogen production – Review. *J Supercrit Fluids* 2018;133:573–90.
- [5] Jin H, Fan C, Wei W, Zhang D, Sun J, Cao C. Evolution of pore structure and produced gases of Zhundong coal particle during gasification in supercritical water. *J Supercrit Fluids* 2018;136:102–9.
- [6] Zhao X, Jin H. Investigation of hydrogen diffusion in supercritical water: a molecular dynamics simulation study. *Int J Heat Mass Transf* 2019;133:718–28.
- [7] Ferreira-Pinto L, Silva Parizi MP, Carvalho de Araújo PC, Zanette AF, Cardozo-Filho L. Experimental basic factors in the production of H₂ via supercritical water gasification. *Int J Hydrogen Energy* 2019;44:25365–83.
- [8] Li Y, Guo L, Zhang X, Jin H, Lu Y. Hydrogen production from coal gasification in supercritical water with a continuous flowing system. *Int J Hydrogen Energy* 2010;35:3036–45.
- [9] Jin H, Lu Y, Liao B, Guo L, Zhang X. Hydrogen production by coal gasification in supercritical water with a fluidized bed reactor. *Int J Hydrogen Energy* 2010;35:7151–60.
- [10] Jin H, Chen Y, Ge Z, Liu S, Ren C, Guo L. Hydrogen production by Zhundong coal gasification in supercritical water. *Int J Hydrogen Energy* 2015;40:16096–103.
- [11] Su X, Jin H, Guo L, Guo S, Ge Z. Experimental study on Zhundong coal gasification in supercritical water with a quartz reactor: reaction kinetics and pathway. *Int J Hydrogen Energy* 2015;40:7424–32.
- [12] Ge Z, Guo L, Jin H. Hydrogen production by non-catalytic partial oxidation of coal in supercritical water: the study on reaction kinetics. *Int J Hydrogen Energy* 2017;42:9660–6.
- [13] Liu Y, Hong W, Cao B. Machine learning for predicting thermodynamic properties of pure fluids and their mixtures. *Energy* 2019;188: 116091.
- [14] Nikolaou ZM, Chen J-Y, Swaminathan N. A 5-step reduced mechanism for combustion of CO/H₂/H₂O/CH₄/CO₂ mixtures with low hydrogen/methane and high H₂O content. *Combust Flame* 2013;160:56–75.
- [15] Hu J, Duan Z, Zhu C, Chou IM. PVTx properties of the CO₂–H₂O and CO₂–H₂O–NaCl systems below 647 K: Assessment of experimental data and thermodynamic models. *Chem Geol* 2007;238:249–67.
- [16] Brodholt JP, Wood BJ. Measurements of the PVT properties of water to 25 kbars and 1600°C from synthetic fluid inclusions in corundum. *Geochem Cosmochim Acta* 1994;58:2143–8.
- [17] Duan Z, Møller N, Weare JH. A general equation of state for supercritical fluid mixtures and molecular dynamics simulation of mixture PVTx properties. *Geochem Cosmochim Acta* 1996;60:1209–16.
- [18] Fenghour A, Wakeham WA, Watson JTR. Densities of (water + carbon dioxide) in the temperature range 415 K to 700 K and pressures up to 35 MPa. *J Chem Thermodyn* 1996;28:433–46.
- [19] Withers AC, Kohn SC, Brooker RA, Wood BJ. A new method for determining the P-V-T properties of high-density H₂O using NMR: results at 1.4–4.0 gpa and 700–1100°C. *Geochem Cosmochim Acta* 2000;64:1051–7.
- [20] Abramson EH, Brown JM. Equation of state of water based on speeds of sound measured in the diamond-anvil cell. *Geochem Cosmochim Acta* 2004;68:1827–35.
- [21] Duan Z, Zhang Z. Equation of state of the H₂O, CO₂, and H₂O–CO₂ systems up to 10 GPa and 2573.15K: molecular dynamics simulations with ab initio potential surface. *Geochem Cosmochim Acta* 2006;70:2311–24.
- [22] Zhang C, Duan Z. A model for C–O–H fluid in the Earth's mantle. *Geochem Cosmochim Acta* 2009;73:2089–102.
- [23] Yang X, Feng Y, Jin J, Liu Y, Cao B. Molecular dynamics simulation and theoretical study on heat capacities of supercritical H₂O/CO₂ mixtures. *J Mol Liq* 2019. 112133.
- [24] Guàrdia E, Martí J. Density and temperature effects on the orientational and dielectric properties of supercritical water. *Phys Rev* 2004;69. 011502.
- [25] Yang X, Duan C, Xu J, Liu Y, Cao B. A numerical study on the thermal conductivity of H₂O/CO₂/H₂ mixtures in supercritical regions of water for coal supercritical water gasification system. *Int J Heat Mass Transf* 2019;135:413–24.
- [26] Yang X, Feng Y, Xu J, Jin J, Liu Y, Cao B. Numerical study on transport properties of the working mixtures for coal supercritical water gasification based power generation systems. *Appl Therm Eng* 2019;162:114228.
- [27] Yang X, Xu J, Wu S, Yu M, Hu B, Cao B, et al. A molecular dynamics simulation study of PVT properties for H₂O/H₂/CO₂ mixtures in near-critical and supercritical regions of water. *Int J Hydrogen Energy* 2018;43:10980–90.
- [28] Duan Z, Møller N, Weare JH. Molecular dynamics simulation of PVT properties of geological fluids and a general equation of state of nonpolar and weakly polar gases up to 2000 K and 20,000 bar. *Geochem Cosmochim Acta* 1992;56:3839–45.
- [29] Berweger CD, van Gunsteren WF, Müller-Plathe F. Force field parametrization by weak coupling. Re-engineering SPC water. *Chem Phys Lett* 1995;232:429–36.
- [30] Berendsen HJC, Grigera JR, Straatsma TP. The missing term in effective pair potentials. *J Phys Chem* 1987;91:6269–71.

- [31] Jorgensen WL, Chandrasekhar J, Madura JD, Impey RW, Klein ML. Comparison of simple potential functions for simulating liquid water. *J Chem Phys* 1983;79:926–35.
- [32] Abascal JLF, Vega C. A general purpose model for the condensed phases of water: TIP4P/2005. *J Chem Phys* 2005;123: 234505.
- [33] Murthy CS, Singer K, McDonald IR. Interaction site models for carbon dioxide. *Mol Phys* 1981;44:135–43.
- [34] Harris JG, Yung KH. Carbon dioxide's liquid-vapor coexistence curve and critical properties as predicted by a simple molecular model. *J Phys Chem* 1995;99:12021–4.
- [35] PJ J, Ilja SJ. Vapor–liquid equilibria of mixtures containing alkanes, carbon dioxide, and nitrogen. *AIChE J* 2001;47:1676–82.
- [36] Buch V. Path integral simulations of mixed para-D₂ and ortho-D₂ clusters: the orientational effects. *J Chem Phys* 1994;100:7610–29.
- [37] Yang Q, Zhong C. Molecular simulation of adsorption and diffusion of hydrogen in Metal–Organic frameworks. *J Phys Chem B* 2005;109:11862–4.
- [38] Guillot B, Guissani Y. A computer simulation study of the temperature dependence of the hydrophobic hydration. *J Chem Phys* 1993;99:8075–94.
- [39] Kong CL. Combining rules for intermolecular potential parameters. II. Rules for the Lennard-Jones (12–6) potential and the Morse potential. *J Chem Phys* 1973;59:2464–7.
- [40] Plimpton S. Fast parallel algorithms for short-range molecular dynamics. *J Comput Phys* 1995;117:1–19.
- [41] Hoover WG. Canonical dynamics: equilibrium phase-space distributions. *Phys Rev A* 1985;31:1695–7.
- [42] Melchionna S, Ciccotti G, Lee Holian B. Hoover NPT dynamics for systems varying in shape and size. *Mol Phys* 1993;78:533–44.
- [43] Seward TM, Franck EU. The system hydrogen - water up to 440°C and 2500 bar pressure. *Berichte der Bunsen-Gesellschaft-Physical Chemistry Chemical Physics* 1981;85:2–7.
- [44] Frost DJ, Wood BJ. Experimental measurements of the properties of H₂O-CO₂ mixtures at high pressures and temperatures. *Geochem Cosmochim Acta* 1997;61:3301–9.
- [45] Tsiklis DSMV, Gavrilov SD, Egorov AN, Timofeeva GV. Molar volumes and equation of state of molecular hydrogen at high pressures. *Dokl Akad Nauk SSSR* 1975;220(6):1384–6.
- [46] Cheng S, Shang F, Ma W, Jin H, Sakoda N, Zhang X, et al. Density data of two (H₂ + CO₂) mixtures and a (H₂ + CO₂ + CH₄) mixture by a modified burnett method at temperature 673 K and pressures up to 25 MPa. *J Chem Eng Data* 2019;64:1693–704.